International Journal of Lightweight Materials and Manufacture 3 (2020) 317–327

Contents lists available at ScienceDirect

International Journal of Lightweight Materials and Manufacture

journal homepage: https://www.sciencedirect.com/journal/international-journal-of-lightweight-materials-and-manufacture

Original Article

Optimization of preparation technology on fibre metal laminates (FMLs) for high-temperature applications

Yubing Hu [a, *], Jin Zhou [b, d], Fan Ji [c], Yanan Zhang [c, **], Yugang Duan [b], Zhongwei Guan [d], Jie Tao [e]

[a] National Special Superfine Powder Engineering Research Center of China, Nanjing University of Science & Technology, Nanjing 210014, China
[b] School of Mechanical Engineering, Xi'an Jiaotong University, Xi'an 710049, China
[c] College of Materials Science & Engineering, Nanjing Tech University, Nanjing 211816, China
[d] School of Engineering, University of Liverpool, Liverpool L69 3GH, UK
[e] College of Material Science and Technology, Nanjing University of Aeronautics and Astronautics, Nanjing 211106, China

ARTICLE INFO

Article history:
Received 2 April 2020
Received in revised form
6 May 2020
Accepted 7 May 2020
Available online 21 May 2020

Keywords:
Fibre metal laminates
Prepreg
Polyimide resin
Surface treatment
Titanium

ABSTRACT

Fibre metal laminates based on titanium and carbon fibre reinforced polyimide (TCP-FML) are designed and manufactured to meet the requirements of high temperature applications. In this work, the preparation technology of the TCP-FML was optimized through the investigation of prepreg manufacture as well as surface treatment of titanium. Prepreg were manufactured using a solution dip method. The effects of step width, fibre tension and translational speed on the performance of prepreg were studied. Surface treatments were performed on titanium using sandblasting, chromic acid (CAA) anodization and NaTESi anodization methods. SEM observation and contact angle were used to analyze the surface characteristics of titanium. The effects of surface treatment on the interlaminar properties of titanium/polyimide were investigated by single-lap shear test and double cantilever beam (DCB) tests. This careful surface preparation, to ensure a good interfacial strength, is crucial for good mechanical properties.

1. Introduction

Fibre metal laminates (FMLs) are a class of hybrid composites consisting of alternating plies of metal and fibre-reinforced polymer [1–3]. Combining the advantages of metal and fibre-reinforced polymer, FMLs exhibit excellent properties such as fatigue and impact resistance. Hence, they have been selected as promising materials in the manufacture of aircraft. With the development of the aerospace industry, aircraft are being designed to fly faster than ever before [4–6]. One of the challenges for the materials is the high temperature due to aerodynamic heating. Therefore, FMLs with high temperature resistance are designed and manufactured to meet the new requirements.

Prepreg refers to "pre-impregnated" composite fibres with a thermoplastic or thermosetting resin. Prepreg is frequently used in the manufacture of composites for structural applications. As an important raw material for manufacturing fibre-reinforced composite structures, the performance of prepreg is closely related to the quality of composite components. Therefore, strictly controlling the preparation process of the prepreg is of a great significance for stabilizing the performance of the prepreg and even the overall performance of the composite material component [7].

According to the definition of prepreg, there are two basic constituents to prepreg, namely the reinforcing fibre and the resin matrix. Regarding the certain resin and fibre, a decision has to be made as to how to apply the resin to the fibre. Nominally there are four methods of impregnation such as solution dip, solution spray, direct hot-melt coat as well as film calendaring [8]. A suitable method should be selected according to the resin system. Besides, the preparation parameters of prepreg also depend on the characteristics of the fibre and the resin, which have significant influence on the quality of prepreg.

FMLs are composed of metal layers and prepreg layers. After curing, the metal is bonded to the fibre-reinforced resin layer. Hence, the bonding strength between the metal and the resin

* Corresponding author.
** Corresponding author.
E-mail addresses: hyb@njust.edu.cn (Y. Hu), zyn3648@163.com (Y. Zhang).
Peer review under responsibility of Editorial Board of International Journal of Lightweight Materials and Manufacture

https://doi.org/10.1016/j.ijlmm.2020.05.001

greatly affects the overall properties of FMLs. In order to produce a strong and durable adhesive joint between metal and resin, surface modifications must be conducted on the metal. There are a wide range of surface treatment methods including mechanical [9,10], chemical [11], electrochemical [12,13] and plasma treatments [14,15] which have been developed to improve the bonding strength between metal and resin. It is important to optimize the surface treatment method for certain metal and resin system.

Based on the discussion above, the main aim of the current study is therefore to optimize the preparation technology of the FMLs based on titanium and carbon fibre reinforced polyimide (TCP-FML) including the fabrication of prepreg, surface treatments of titanium and curing of laminates. The preparation of carbon fibre reinforced polyimide prepreg was discussed. The effects of step width, fibre tension and translational speed on the performance of prepreg are explored. Then, the effects of titanium surface treatment on the interlaminar bonding strength were studied in detail.

2. Materials and experimental procedures

2.1. Materials

PMR type polyimide resin (KH 308) was purchased from the Institute of Chemistry, the Chinese Academy of Science of China. Carbon fibres were TR50S 6L provided by Mitsubishi Rayon Co. Ltd., Japan. Titanium (TA2 grade) with a 0.3 mm thickness was purchased from BaoJi Titanium Industry Co. Ltd., China. Table 1 shows the main performance parameters of carbon fibre. The chemical composition and content of the titanium alloy (TA2) are shown in Table 2. The layout equipment is PBJ-13 SKPL2-500, which is a layout machine developed by Xi'an Longde Technology Development Co., Ltd., as shown in Fig. 1.

2.2. Manufacture of carbon fibre/polyimide prepreg

In the current study, PMR type polyimide is an ethanol solution when uncured. Therefore, the carbon fibre reinforced PMR polyimide prepreg was prepared by a solution dip method on a numerical control fibre winding machine as shown in Fig. 1. During the preparation of prepreg, the release paper was firstly laid on the surface of the roller. Then, the carbon fibres were passed through each of the yarn spreading rollers and the dipping tank in sequence and fixed to the edge of the release paper. The arrangement parameters, such as the translational speed, step width and fibre tension, were set. Next, through the equipment, the carbon fibres were passed through the resin solution in the dipping tank at a uniform speed and arranged on the release paper side by side. Finally, the prepreg was cut along the roller busbar and removed and dried in a cool place. The setting parameters during prepreging is shown in Table 3.

Table 3
Parameter setting during prepreg preparation.

Parameter	Step width (mm)	Fibre tension (N)	Translational speed (m/min)
Setting	3.6/3.7/3.8	4/7/10/13	10/14/18/22/26

2.3. The method for evaluating prepreg performance

The evaluation of prepreg in this experiment is carried out from the following two aspects:

(1) Surface quality of prepreg

Observing whether there are defects in the appearance of the prepreg, that is: the surface is flat, seamless, with no fibre bundles overlap, no fibre skew and no side inconsistencies.

(2) Fibre volume content of prepreg

The resin in the prepreg was completely dissolved by putting the sample in an ethanol solvent, and the volume content of the fibre in the prepreg was calculated by measuring the mass change before and after the dissolving process.

Table 1
The main performance parameters of the selected carbon fibre.

Performance	Diameter (μm)	Weight (mg/m)	Tensile strength (MPa)	Young's modulus (GPa)	Elongation (%)	Density g/cm^3
TR50S 6L	7	400	4900	240	2	1.82

Table 2
The chemical composition and content of TA2.

Element	Fe	C	N	H	O	Non-titanium	Ti
Content (wt%)	≦0.30	≦0.08	≦0.03	≦0.015	≦0.25	≦0.40	margin

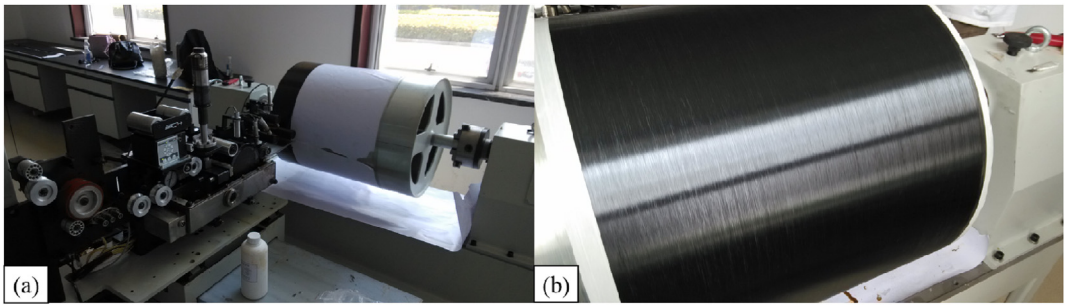

Fig. 1. Prepreg preparation and layout machine.

2.4. Optimization of prepreg preparation process

2.4.1. Effect of step width on prepreg quality

The setting of the step width parameter controls the forward speed of the unit (along the direction of the roller busbar). Ideally, during the time of a single revolution of the carbon fibre winding drum, the unit can shift a distance of step width. The proper setting of the step width can ensure that there are no gaps between two adjacent yarns and there is no serious yarn overlap. The step width has a direct relationship to the width of the carbon fibre bundle and the yarn spreading performance of the equipment. During the preparation process, three sets of parameters were designed with step widths of 3.6, 3.7 and 3.8 mm.

The experimental results showed that when the step width was 3.6 mm, the prepreg stacking rate was large, while the thickness uniformity of the prepreg was unacceptable. Gaps between two adjacent fibres were observed when the step width was set to 3.8 mm, which would affect the performance of the prepreg. When the step width was set to 3.7 mm, the prepared prepreg showed a small stacking rate and a smooth surface condition. It should be noted that the setting of the step width parameter is related to the performance of the carbon fibre grade. In terms of the carbon fibre used in this experiment, the thickness uniformity of the prepreg prepared with the step width parameter set to 3.7 mm is relatively high, and there is no obvious gap between the two adjacent bundles of fibres.

2.4.2. Influence of fibre tension on prepreg quality

Fibre tension is another important parameter that affects the performance of the prepreg during the manufacture. If the tension is too low, the prepared prepreg will not be dense enough and the strength of the product will be reduced. Conversely, if the tension is too large, the fibres are prone to abrasion, resulting in reduced strength and even fibre breakage. As a result, a “fluff” phenomenon occurs on the surface of the prepreg, which seriously affects the surface quality and strength of the prepreg. Similarly, the setting of the fibre tension is related to the carbon fibre specifications.

For the carbon fibres used in this experiment, when the fibre tension is 4–7 N, the surface of the prepared prepreg is uniform and the surface is free of fluff. When the fibre tension exceeds 10 N, the fibre breakage during the preparation process will be severe and therefore, the quality of the prepared prepreg is poor.

2.4.3. Influence of translational speed on the quality of prepreg

The relationship between the translational speed and the fibre volume content in the prepared prepreg is shown in Fig. 2. As the translational speed increases, the fibre volume content in the prepreg also increases. During the preparation of the prepreg, the translational speed mainly affects the dipping process of the fibre. The faster the translational speed, the shorter the contact time between the fibre and the resin, and the higher the volume content of the fibre in the prepreg produced. Since the reinforcing fibre is the main carrier of the force in the composite material, a high fibre volume content will help to improve the mechanical properties of the composite component. However, fibre volume content is not to be as high as possible. There is an optimal ratio between the resin matrix and the fibre-reinforced material.

It can be seen from Fig. 2 that when the translational speed is set to 22 m/min, the volume content of the prepared prepreg fibre is about 50%, which can better meet the actual production process requirements.

2.5. Surface treatment of titanium

Fibre metal laminate is made of metal sheet and fibre-reinforced composite material by alternating hot press curing. In addition to the adhesion between the fibre and the resin matrix, the adhesion force between the resin matrix and the metal plate affects the performance of the overall mechanical properties of the laminate. Before the preparation of fibre metal laminates, the surface of the metal sheet should be pre-treated to construct the surface microstructure conducive to bonding, in order to improve the bonding force of the interface layer between the metal and the composite material and the environmental durability of the laminates [16]. In this work, three kinds of surface treatment technologies were performed on titanium, i.e. sandblasting, NaTESi [17] anodization and chromic acid (CAA) anodization [18]. The effects of these three treatments were compared.

2.5.1. Sandblasting treatment

Brown corundum sand with a diameter of about 100 μm was used to perform the sandblasting treatment. The sample surface was sandblasted under 0.55 MPa pressure with an airbrush to ensure the surface sandblasted evenly. After sandblasting, the samples were ultrasonically cleaned in acetone until all oil stains were removed. Subsequently, the samples were cleaned with deionized water and dried in the atmosphere.

2.5.2. NaTESi anodization

The surface of titanium can be contaminated by oil and other impurities during the production, storage and transportation processes, which can adhere to the surface of titanium and block its contact with electrolyte. On the other hand, these pollutants can be dissolved in electrolyte, resulting in an adverse effect on the experiment. Therefore, before anodization, titanium was cleaned with tap water to remove any visible dust on its surface, and then it was further cleaned with acetone and other organic solvents to remove any oil stains on its surface. After being cleaned in this way the titanium was then transferred to a nitric acid/hydrofluoric acid mixture (nitric acid: 350 g/L, hydrofluoric acid: 60 g/L) for pickling to remove the oxide film on the surface. Finally, the titanium was cleaned with deionized water to remove the remaining acid.

NaTESi anodization was performed on titanium with a voltage of 10 V for 10 min using an electrolyte containing 300 g/L sodium hydroxide, 65 g/L Na-tartrate, 30 g/L ethylene diamine tetra acetic acid (EDTA) and 6 g/L Na_2SiO_3. After anodization, the samples were cleaned with de-ionized water and dried in the atmosphere. A schematic of the anodizing setup is shown in Fig. 3.

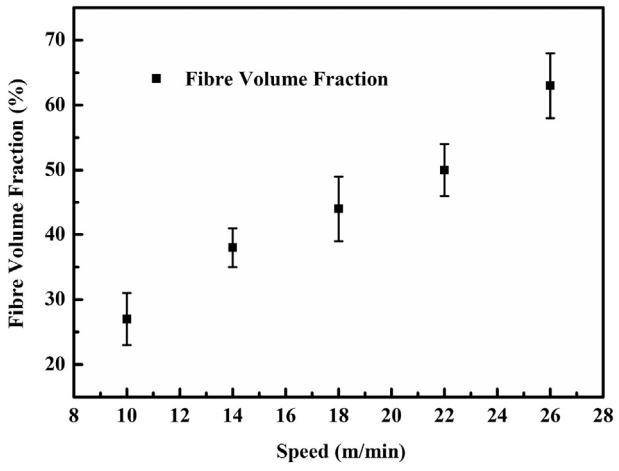

Fig. 2. Relationship between translational speed and fibre volume content of prepreg.

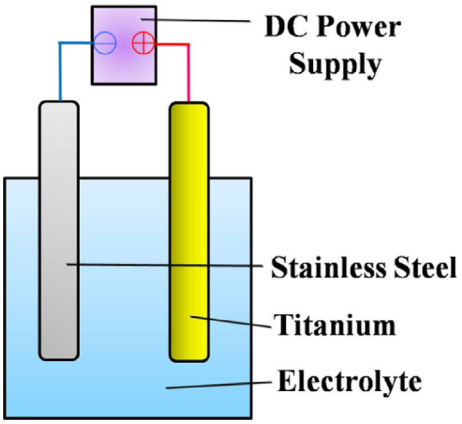

Fig. 3. Schematic of the anodizing setup.

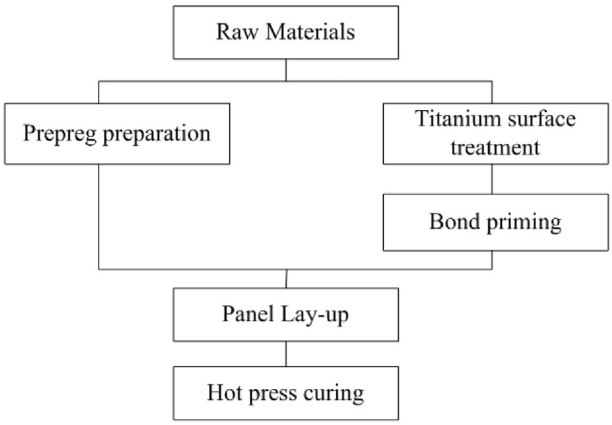

Fig. 4. Preparation process of TCP-FML.

2.5.3. CAA anodization

Similar to the process of NaTESi anodization, titanium was firstly cleaned with acetone and mixed acid. After that, the titanium was submerged into an electrolyte solution including chromium oxide 5 g/L and hydrofluoric acid 0.1 g/L. Then, the anodization was conducted at a voltage of 10 V for 20 min. After the electrodeposition, the samples were removed from the electrolyte, washed with deionized water, and dried after cleaning the electrolyte on the surface.

2.6. Curing of FMLs by compression molding

The process route for preparing TCP-FML by compression molding is shown in Fig. 4. In order to increase the interfacial bonding between the metal and the prepreg, a layer of KH-308 resin was applied as a primer on the metal surface after the surface treatment. The titanium and prepreg were alternately placed into the mold and cured according to the process shown in Fig. 5. Specific curing steps are: heating to 80 °C for 60 min, heating to 120 °C for 60 min, heating to 160 °C for 60 min, heating to 200 °C and then applying contact pressure for 60 min. Again heating to 280 °C, pressurization and deflation several times, and then maintaining a pressure of 1.5~2 MPa, heating to 320 °C, holding for 2 h, cooling within a furnace, and finally maintaining pressure at 1.5~2 MPa.

The KH-308 resin used in the experiment is an ethanol solution of polyamic acid, which has not been imidized. During the curing of the FMLs, the reaction process of the resin matrix is shown in Fig. 6. It can be seen that the resin will produce small molecular substances during the curing process, and if the generated small molecules cannot be discharged in time, they will become voids inside the material after curing, which will seriously affect the performance of the material. Therefore, in order to ensure the overall performance of the material, it is necessary to discharge the generated small molecules as much as possible when formulating the curing process. In order to reduce the porosity of the material and ensure the homogeneity of the resin in the system, an appropriate temperature rise curve and pressure point must be selected. In this study, the gradient heating method is used to heat the system in order to prevent excessive resin outflow caused by rapid volatilization of the solvent, resulting in uneven resin distribution inside the material. When selecting the pressure point, it is necessary to consider the reaction characteristics of the resin. When the temperature of the selected pressure point is too low, the viscosity of the system is large, which is not conducive to the dispersion of the resin and the release of small molecules. If the selected temperature is too high, the processing time window will be shortened as the resin cross-linking reaction proceeds. Premature pressing time will affect the release of small molecules formed by imidization after pressing, resulting in high porosity of the system. If the pressure is applied too late, it will be difficult to compact because the degree of crosslinking of the system is too high, and the prepared material will have high porosity. In this work, the curing parameter is selected according to our previous work [4].

2.7. Characterization

Microstructures of the specimens were observed under a field emission scanning electron microscope (FE-SEM, Hitachi S4800, Japan). An optical contact angle meter (JC2000D7M, Zhong Chen Ltd., Shanghai) was used to analyze the static wetting performance of the sample surface. The measurement accuracy was ±0.1°. The droplet volume used was 3 μL. In addition, the circular contact method was used to calculate the apparent contact angle (APCA, Apparent contact angle) of the droplets in the optical picture. The test results are based on the average of the three repeatedly measured data.

The single-lap shear test was used to evaluate the strength of the titanium/polyimide adhesive joint, so as to further analyze the effect of the titanium surface treatment. The preparation of single-lap shear specimens is performed with reference to ASTM D1002. The dimensions of the specimen is shown in Fig. 7. The experiment was completed on a SANS CMT 5105 electronic universal testing machine. During the test, the load was performed at a speed of 2 mm/min under the environment of 20–30 °C until the sample was sheared off. Calculation of the tensile shear strength τ of the titanium/polyimide joint was done by the following formula,

$$\tau = \frac{P}{S} \tag{1}$$

where P is the load when the specimen fails, and S is the area of the bonding surface. During the experiment, each sample was repeated three times and an average value was taken.

In order to reflect the bonding performance between resin/metal interface, pure mode I interlaminar fracture toughness (G_{Ic}) tests were performed on double cantilever beam (DCB) specimens in accordance with the standard HB7718.1. The geometric dimensions of the sample and clamping method are shown in Fig. 8. The experimental loading rate is 2 mm/min and the unloading rate is 5 mm/min. The G_{Ic} is calculated using the following equation:

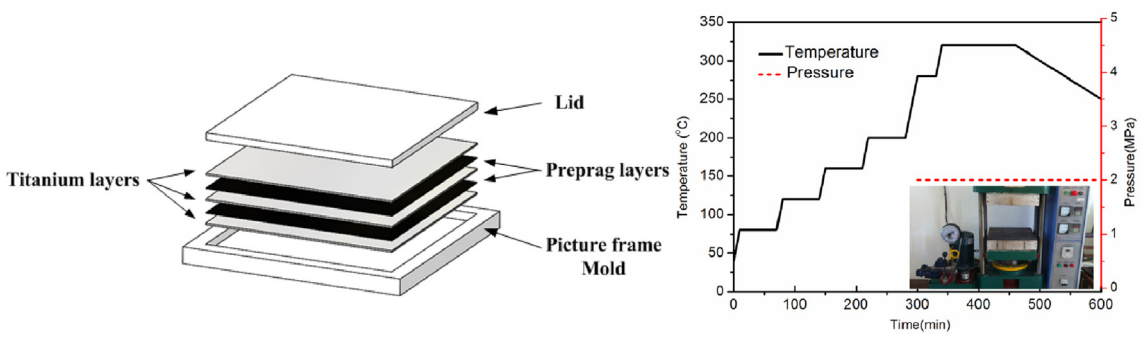

Fig. 5. Schematic of lay-up and Curing process of TCP-FML.

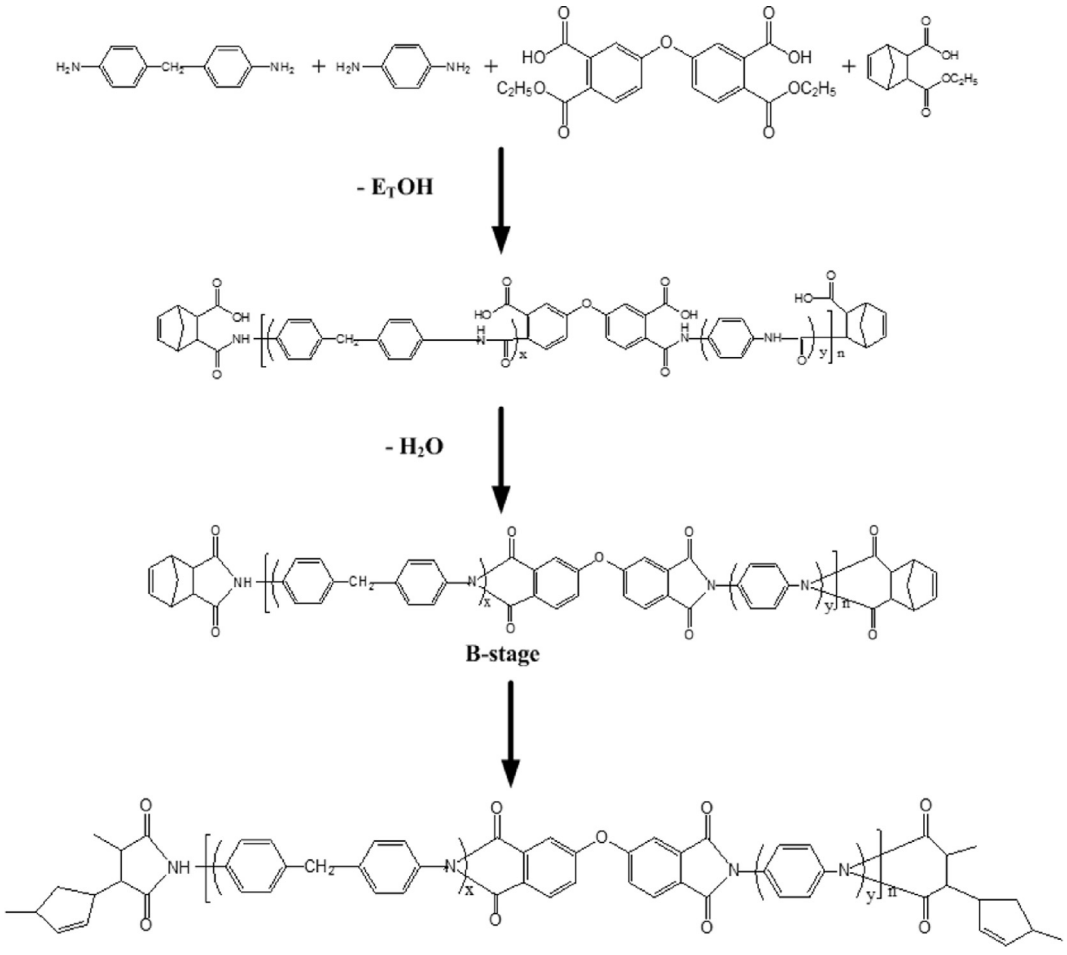

Fig. 6. Chemical process of KH-308 resin curing.

$$G_{Ic} = \frac{mP\delta}{2a'W} \times 10^3 \tag{2}$$

Here, G_{Ic} is the interlaminar fracture toughness, m is the fitting coefficient of the flexibility curve. P is the critical load of the initial crack propagation between layers. δ is the elastic opening displacement at the loading point corresponding to P. a' is the crack length. W is the average width of the specimen.

The fitting coefficient of the flexibility curve of a single sample is calculated as follows:

$$m = \frac{\sum_{i=1}^{K} \log a_i \log C_i - \frac{1}{K}\left(\sum_{i=1}^{K} \log a_i\right)\left(\sum_{i=1}^{K} \log C_i\right)}{\sum_{i=1}^{K} (\log a_i)^2 - \frac{1}{K}\left(\sum_{i=1}^{K} \log a_i\right)^2} \tag{3}$$

where a_i is the crack length before the i-th loading. C_i is the sample flexibility, $C_i = \delta_i/P_i$, K is the number of measurement points for a single sample.

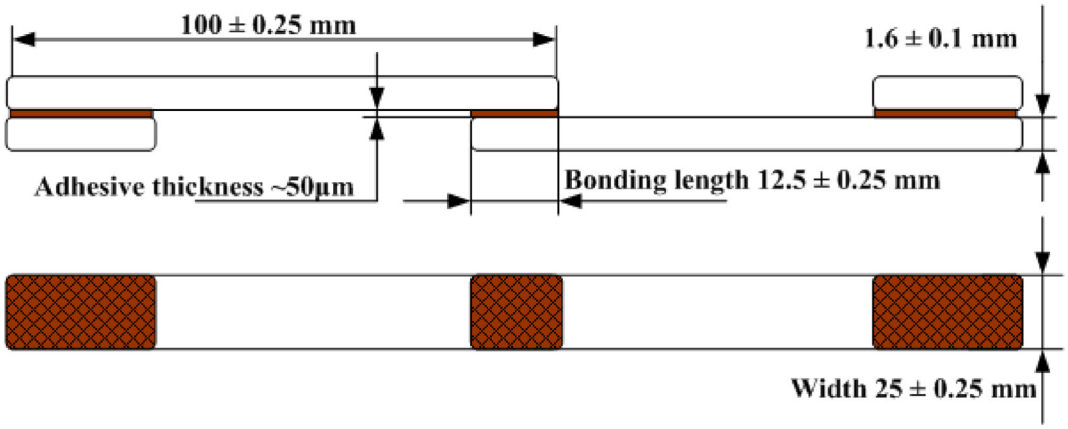

Fig. 7. Dimensions of Single-lap shear sample.

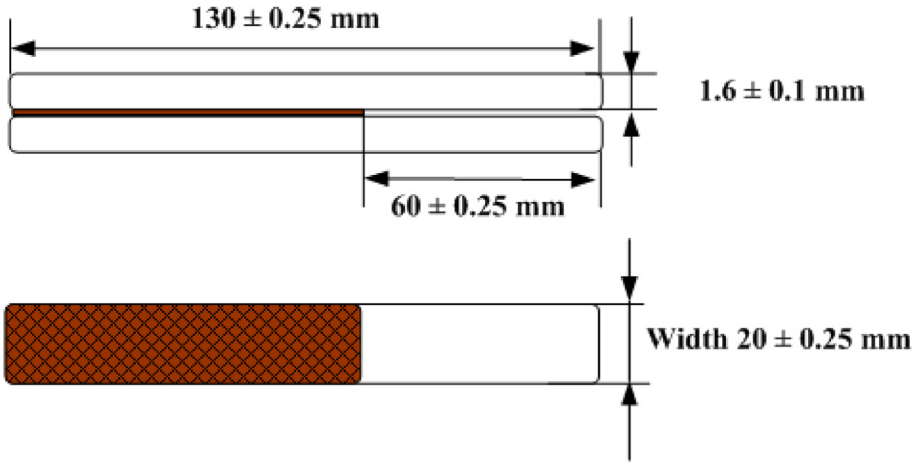

Fig. 8. Dimensions of the samples and clamping method of the DCB test.

3. Results and discussion

3.1. Effect of surface treatment on the surface morphology of titanium

After surface treatments with different methods, the surface morphology and surface structure of the titanium changed significantly. Fig. 9 is a scanning electron microscope photograph of the surface of the titanium which was treated with different processes. The schematic diagram when the titanium is bonded to the resin is shown in Fig. 10. It shows that the surfaces of the titanium, after the treatment, have formed an uneven surface structure. Compared with the untreated titanium (Fig. 9a), the surface roughness of the treated titanium has been increased, which has an important effect on improving the bonding strength between the titanium and the resin. In fact, the bonding between metal and resin mainly depends on the "micromechanical bonding" and "physical-mechanical interlocking" between them. By increasing the contact area between metal and resin, the bonding strength between the two can be improved. It can be seen that the surface of the titanium, after sandblasting, had formed a micron-level rough structure, and its surface area had been increased to a certain extent compared to the untreated titanium. After the surface treatment of the titanium by an electrochemical anodization method, an oxide layer was formed on the surface of the titanium substrate, and there were a large number of holes with a pore diameter of several nanometres, which effectively improved the contact area between the titanium and the resin. Therefore, compared with sandblasting, the anodizing method can produce a larger specific surface area on the surface of the substrate of the titanium, resulting in a better interface property between titanium and polyimide. At the same time, it can be observed that the hole density of the oxide film obtained by NaTESi anodizing treatment is greater than that by CAA method, which plays an important role in improving the mechanical locking force between the titanium and the resin.

3.2. Effect of surface treatment on wetting properties of TA2 surface

Fig. 11 shows the measurement results of the contact angle between the titanium surface and water after different surface treatments. It can be seen from the figure that the apparent contact angle between the untreated titanium surface and water was large, and that between the titanium surface and water after the surface treatment has a significant down-trend. Among them, the contact angle of the samples treated with CAA anodizing and NaTESi anodizing decreased significantly. Similarly, when a resin solution was used as a test solution, the apparent contact angle between the surface of the treated sample and the resin solution has a tendency to decrease compared to the untreated sample, as shown in Fig. 12. The apparent contact angle test results using two different solutions were listed in Table 4. According to the theory of infiltration thermodynamics, when a liquid infiltrates another solid to reach an

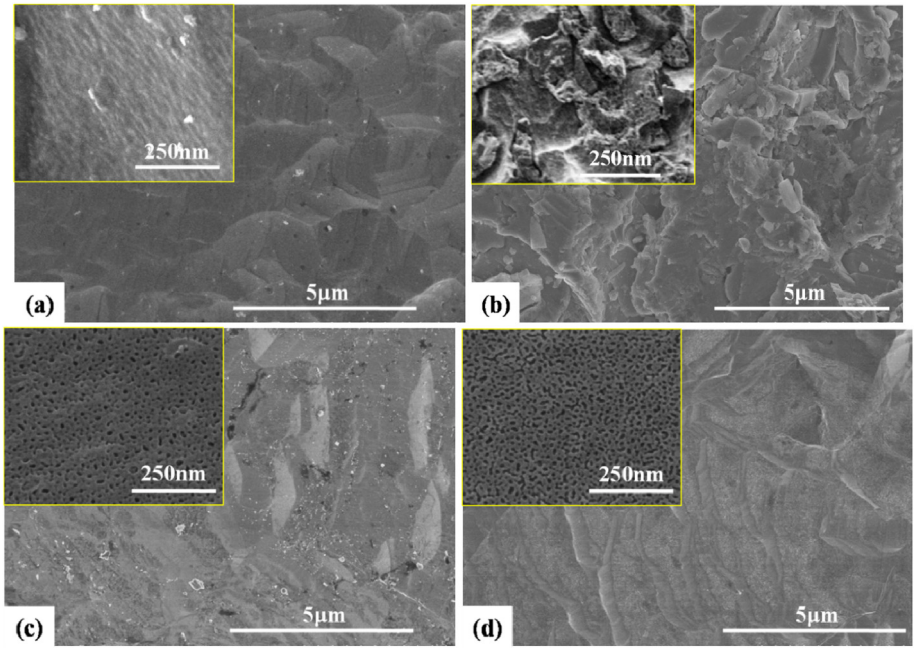

Fig. 9. Surface morphologies of titanium. (a) Neat sample (b) sandblasting (c) CAA anodization (d) NaTESi anodization.

equilibrium state, the relationship of the solid-liquid contact angle and the thermodynamic bonding work (W) and the three-phase interface tension involved satisfy the Young-Dupre equation [19,20]:

$$\cos\theta = (\gamma_S - \gamma_{SL}) / \gamma_L \tag{4}$$

$$W = \gamma_L(1 + \cos\theta) \tag{5}$$

Among them, γ_S is the solid surface tension, γ_L the liquid surface tension, γ_{SL} the solid-liquid interface tension. When the thermodynamic bonding work is at its maximum, the corresponding interface bonding strength is at the highest, and the wettability of the liquid to the solid is the best at this time. Therefore, the smaller the contact angle of a liquid with a solid material, the better its wettability and the higher the interfacial bonding strength.

3.3. *Effect of surface treatment on tensile shear strength of titanium/polyimide interface*

Fig. 13 exhibits the results of single-lap shear tests. By calculating the area enclosed by a load-displacement curve, the work of fracture during the single-lap shear test was obtained. It can be seen that the load increases linearly with the displacement initially

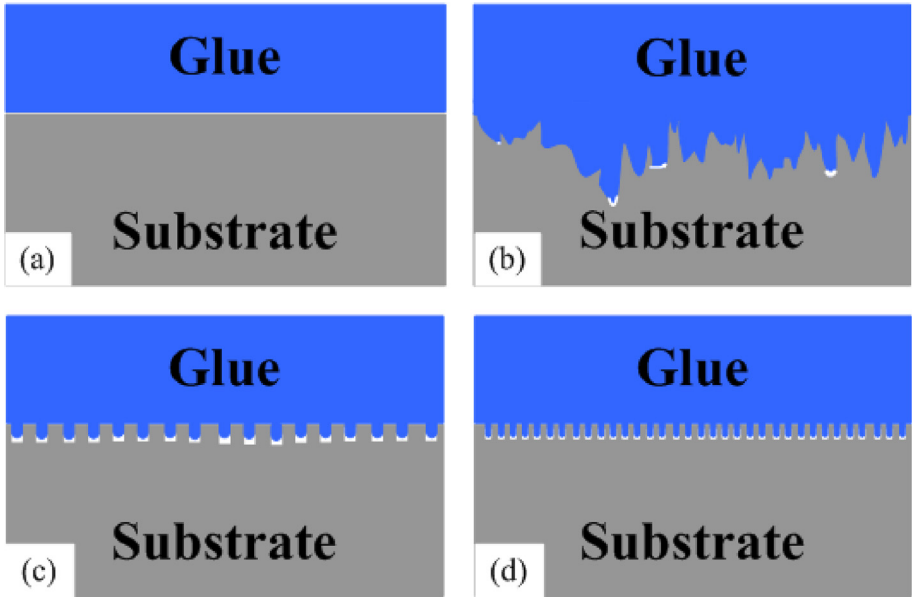

Fig. 10. Schematic of Titanium/resin interface. (a) Neat sample (b) sandblasting (c) CAA anodization (d) NaTESi anodization.

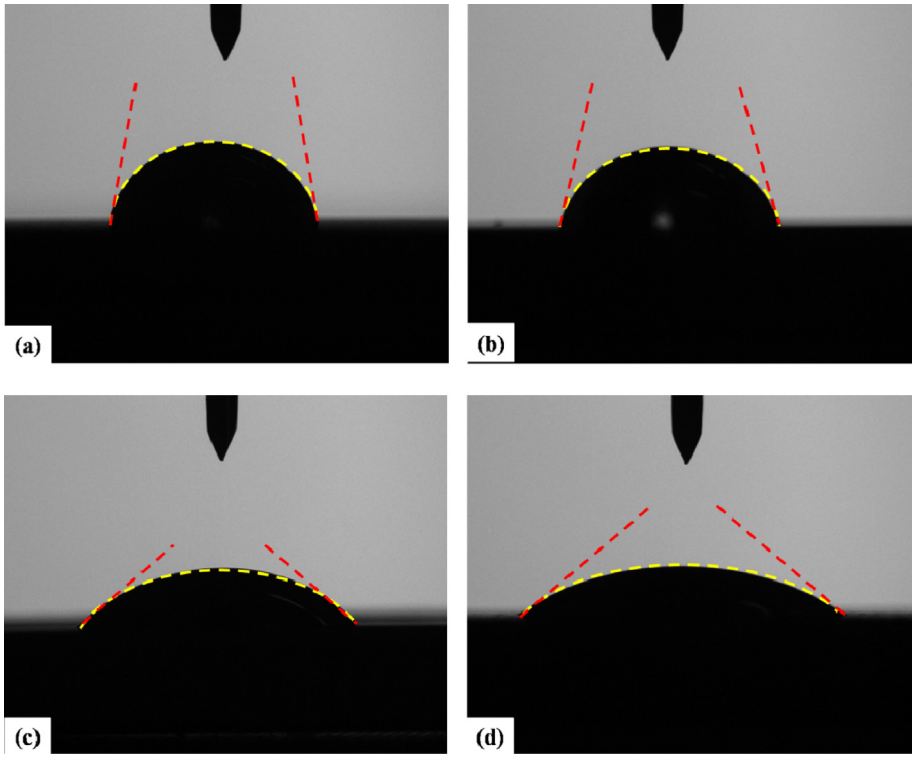

Fig. 11. Static contact angle of titanium surface and water after surface treatment. (a) Neat sample (b) sandblasting (c) CAA anodization (d) NaTESi anodization.

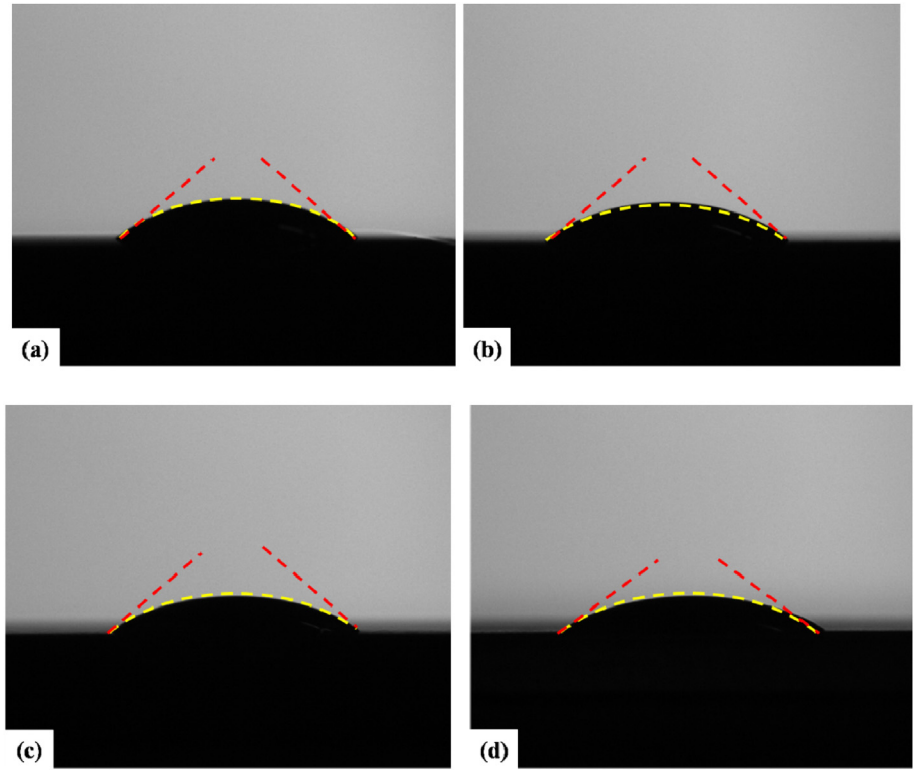

Fig. 12. Static contact angle of titanium surface and resin solution after surface treatment. (a) Neat sample (b) sandblasting (c) CAA anodization (d) NaTESi anodization.

corresponding to the elastic deformation stage of polyimide. Then the load-displacement curve enters a non-linear region, and this section contains the plastic deformation, cohesive failure and interface debonding of polyimide [21]. It was also observed that after surface treatment the titanium/polyimide interface could withstand a higher tensile shear load than the untreated sample.

With the surface treatment, the single-lap shear strength of the sample was greatly improved compared with the untreated sample.

Table 4
Apparent contact angle measurement results.

Surface treatment method	Untreated	Sandblasting	CAA anodizing	NaTESi anodizing
Contact angle with water/(°)	76.7 ± 1.8	67.7 ± 1.5	48.5 ± 1.2	32.1 ± 1.5
Contact angle with resin/(°)	41.2 ± 1.1	37.3 ± 1.3	33.7 ± 1.1	30.6 ± 1.3

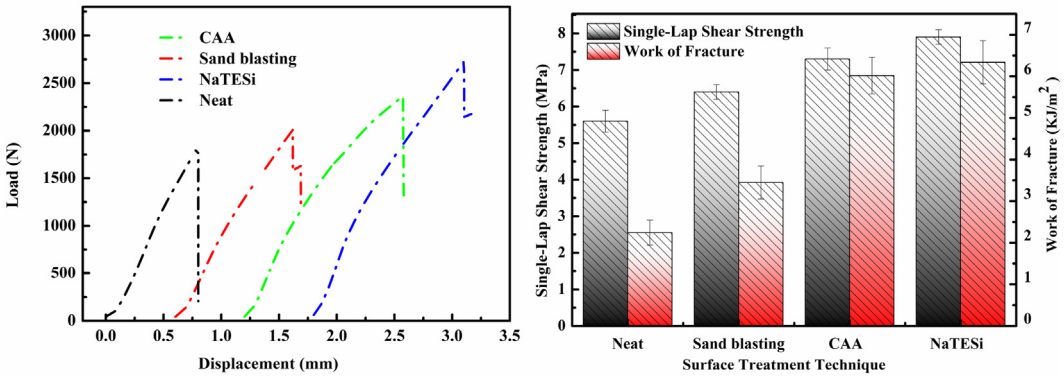

Fig. 13. Single-lap shear test results.

Due to the improvement of the surface roughness of titanium after surface treatment, it is easier to form a mechanical lock between the polyimide and titanium. In addition, the surface of the anodized titanium produces an oxide film whose main component is TiO_2, while the TiO_2 surface easily adsorbs hydroxyl groups. When the titanium is bonded to the polyimide resin, it is easy to generate hydrogen bonding with the carbon-oxygen double bond on the polyimide molecular chain, which further improves the bonding strength, as indicated in Fig. 14. Compared with the untreated titanium, the single-lap shear strengths of the samples treated by sandblasting, CAA anodizing and NaTESi anodizing were increased by 15%, 30%, and 41%, respectively. Similarly, compared to the untreated titanium, the work of fracture of the specimens treated with sandblasting, CAA anodizing treatment and NaTESi anodizing treatment increased by 53%, 166% and 182% during the single-lap shear tests, respectively. This is due to the increase in the specific surface area of the titanium after surface treatment. When an external load is applied, the path of crack growth increases, and a more fresh surface area is generated when the bonding surface is destroyed, which requires a large amount of energy to propagate the crack. Therefore, the work of fracture after surface treatment has been greatly improved (see Table 5).

3.4. Effect of surface treatment on G_{Ic} of titanium/polyimide interface

The measurement results of the G_{Ic} calculated according to equation (2) and equation (3) are shown in Table 6. From the analysis of the data, it can be seen that the G_{Ic} of the titanium/polyimide interface after surface treatment is greatly improved compared to the untreated titanium surface. Compared with the untreated titanium surface, the G_{Ic} of the titanium/polyimide interface after sandblasting, CAA anodizing and NaTESi anodizing treatments were increased by 67%, 73% and 87%, respectively. The failure modes of metal-resin bonded joints include adhesion failure, cohesive failure and their mixed failure, as shown in Fig. 15. The failure forms of the DCB sample in this experiment are shown in Fig. 16. From Fig. 16a, we can see that the surface of the layered failure area of the untreated sample is smooth, and the failure is mainly concentrated at the titanium-polyimide interface, which showed an adhesive failure form. It proves that the bond between the titanium and polyimide resin is weak and when an external force is applied, cracks are easily generated and propagated at this interface. After the surface treatment, the sample showed a mixed failure mode of adhesion failure and cohesive failure. In the mixed

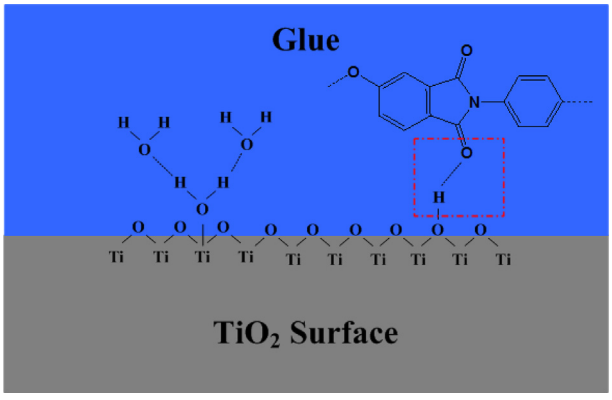

Fig. 14. Schematic diagram of hydrogen bond.

Table 5
Tensile and shear test results of different surface treatment samples.

Sample	Single-Lap shear strength (MPa)	Work of fracture (kJ/m^2)
Untreated	5.61 ± 0.31	2.25 ± 0.32
Sandblasting	6.47 ± 0.32	3.45 ± 0.46
CAA	7.32 ± 0.43	6.02 ± 0.42
NaTESi	7.93 ± 0.25	6.34 ± 0.52

Table 6
DCB experimental results.

Sample code	G_{Ic} measured values (J·m^{-2})			Average value (J·m^{-2})
Untreated	41.13	32.23	39.88	37.75
Sandblasting	65.33	64.98	58.62	62.98
CAA	60.97	68.33	66.21	65.17
NaTESi	75.98	68.80	66.91	70.56

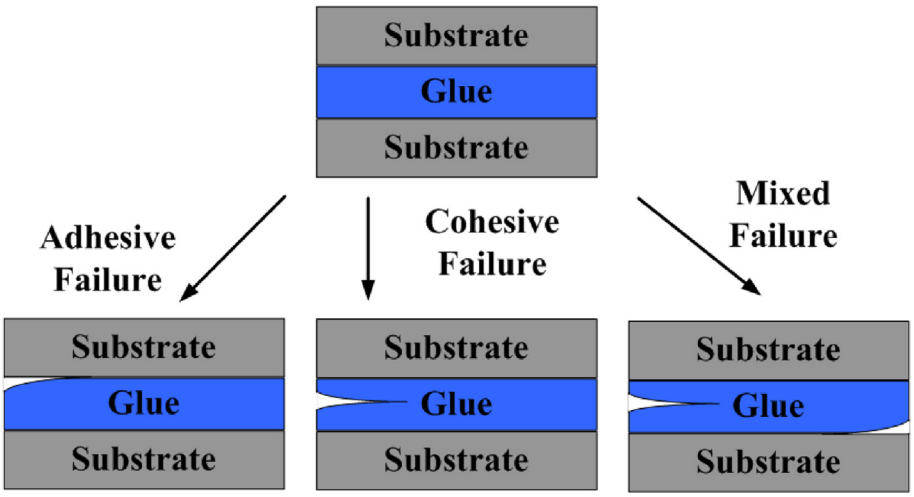

Fig. 15. Schematic diagram of Interface failure mode.

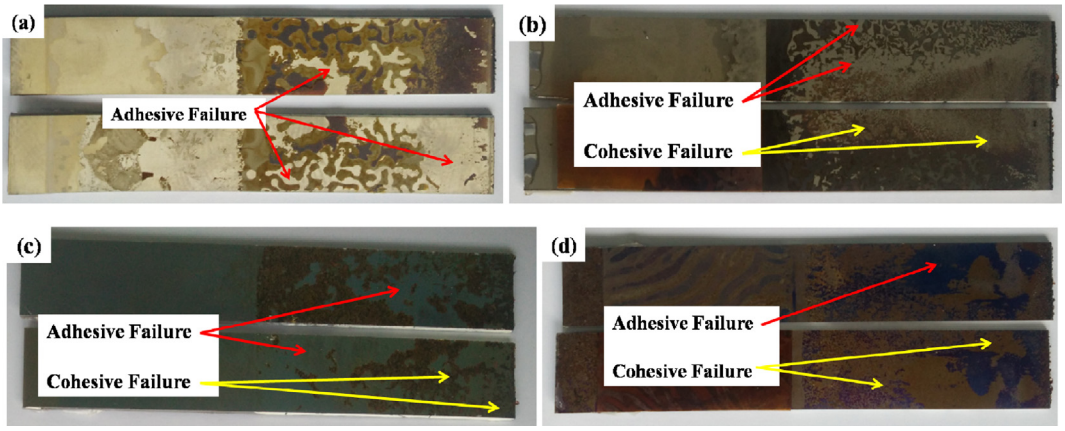

Fig. 16. Failure mode of DCB test. (a) Neat sample (b) sandblasting (c) CAA anodization (d) NaTESi anodization.

failure mode, the crack produces a fresher surface during the propagation. Sandblasting forms a micron-sized rough structure on the surface of the titanium plate, which is beneficial to an increase in the contact area between the titanium and the polyimide resin during bonding, thereby enhancing the mechanical locking and improving its ability to resist delamination and crack propagation when subjected to external forces. Anodizing treatment can produce nano-scale rough morphology on the surface of titanium and its specific surface area is further improved in comparison to that of the sandblasted surface. It can provide more contact area when bonding with polyimide resin, which improves its interface adhesion performance further to a certain extent. In addition, it can be seen from Fig. 9 that the anodized titanium surface produces a loose and porous structure. When bonding with polyimide resin, the resin is embedded in these holes like pins. When subjected to external force to produce a layered expansion, these pins also break down the stress concentration effect of the crack tip in the interface layer at the same time, so that the titanium-polyimide interface can absorb more energy during the crack propagation. Clearly, the denser the surface holes generated, the more obvious its "enhancement" effect. Therefore, the samples treated with NaTESi anodizing have higher G_{Ic} than the samples treated with CAA anodizing. In addition, the hydroxyl groups on the surface of the titanium dioxide oxide film generated during the anodizing process are liable to generate hydrogen bonding with the carbon-oxygen double bond in the polyimide resin, which also improves the interface bonding strength between titanium and polyimide as well as the G_{Ic} value.

4. Conclusions

In summary, the preparation technology of lightweight TPC-FML was optimized by the preparation of prepreg and the surface treatment of titanium. In terms of the PMR type polyimdie (KH-308) and carbon fibre (TR50S 6L), the selected parameters to prepare prepreg are as follows, step width is set to 3.7 mm, fibre tension is 4–7 N, and translational speed is set to 22 m/min. The surface quality of the prepreg prepared under this parameter is excellent, and the fibre volume content is about 50%.

Surface treatment can greatly improve the interfacial adhesion performance between titanium and polyimide. The single-lap shear strength of titanium-polyimide joints using sandblasting, CAA and NaTESi anodizing treatments is increased by 15%, 30% and 41%, respectively, compared to the untreated samples. The work of fracture is increased by 53%, 168% and 182%, respectively, and G_{Ic} increased by 67%, 73% and 87%, respectively.

By employing careful surface preparation, to ensure a good interfacial strength, this confers on these materials with very good mechanical properties.

Conflict of interest

The authors declare that there is no conflicts of interest.

Acknowledgements

The authors gratefully acknowledge the financial support of the Natural Science Foundation of Jiangsu Province (BK20180495, BK20180698).

References

[1] C. Ji, B. Wang, J. Hu, et al., Effect of different preparation methods on mechanical behaviors of carbon fibre-reinforced PEEK-Titanium hybrid laminates, Polym. Test. (2020) 106462.
[2] L. Che, G. Fang, Z. Wu, et al., Investigation of curing deformation behavior of curved fibre metal laminates, Compos. Struct. 232 (2020) 111570.
[3] N.G. Gonzalez-Canche, E.A. Flores-Johnson, J.G. Carrillo, Mechanical characterization of fiber metal laminate based on aramid fiber reinforced polypropylene, Compos. Struct. 172 (2017) 259–266.
[4] Y.B. Hu, H.G. Li, L. Cai, et al., Preparation and properties of Fibre–Metal Laminates based on carbon fibre reinforced PMR polyimide, Compos. B Eng. 69 (2015) 587–591.
[5] Y. Hu, Y. Zhang, X. Fu, et al., Mechanical properties of Ti/CF/PMR polyimide fiber metal laminates with various layup configurations, Compos. Struct. 229 (2019) 111408.
[6] Y. Hu, H. Li, X. Fu, et al., Hygrothermal characterization of polyimide–titanium-based fibre metal laminate, Polym. Compos. 39 (8) (2018) 2819–2825.
[7] Y.D. Huang, L. Liu, Z.Q. Zhang, et al., On-line monitoring of resin content for film impregnation process, Compos. Sci. Technol. 58 (9) (1998) 1531–1534.
[8] M. Molyneux, P. Murray, B.P. Murray, pre-preg, tape and fabric technology for advanced composites, Composites 14 (2) (1983) 87–91.
[9] Y.W. Kim, Surface modification of Ti dental implants by grit-blasting and micro-arc oxidation, Mater. Manuf. Process. 25 (5) (2010) 307–310.
[10] D. Lakstein, W. Kopelovitch, Z. Barkay, et al., Enhanced osseointegration of grit-blasted, NaOH-treated and electrochemically hydroxyapatite-coated Ti–6Al–4V implants in rabbits, Acta Biomater. 5 (6) (2009) 2258–2269.
[11] H.C. Man, N.Q. Zhao, Z.D. Cui, Surface morphology of a laser surface nitrided and etched Ti–6Al–4V alloy, Surf. Coating. Technol. 192 (2–3) (2005) 341–346.
[12] P. He, K. Chen, J. Yang, Surface modifications of Ti alloy with tunable hierarchical structures and chemistry for improved metal–polymer interface used in deepwater composite riser, Appl. Surf. Sci. 328 (2015) 614–622.
[13] Z. Liu, H. Liu, X. Zhong, et al., Characterization of anodic oxide growth on commercially pure titanium in NaTESi electrolyte, Surf. Coating. Technol. 258 (2014) 1025–1031.
[14] Y. Lin, H. Li, Q. Wang, et al., Effect of plasma surface treatment of aluminum alloy sheet on the properties of Al/Gf/PP laminates, Appl. Surf. Sci. 507 (2020) 145062.
[15] M. Akram, K.M.B. Jansen, L.J. Ernst, et al., Atmospheric plasma modification of polyimide sheet for joining to titanium with high temperature adhesive, Int. J. Adhesion Adhes. 65 (2016) 63–69.
[16] R.D. Adams, J. Comyn, W.C. Wake, Structural Adhesive Joints in engineering, Springer Science & Business Media, 1997.
[17] Y.S. Yu, L.S. Xie, M.H. Chen, et al., Surface characteristics and adhesive strength to epoxy of three different types of titanium alloys anodized in NaTESi electrolyte, Surf. Coating. Technol. 280 (2015) 122–128.
[18] E. Matykina, I. García, J.J. De Damborenea, et al., Comparative determination of TiO2 surface free energies for adhesive bonding application, Int. J. Adhesion Adhes. 31 (8) (2011) 832–839.
[19] H.J. Butt, D.S. Golovko, E. Bonaccurso, On the derivation of Young's equation for sessile drops: nonequilibrium effects due to evaporation, J. Phys. Chem. B 111 (19) (2007) 5277–5283.
[20] Y. Xiu, L. Zhu, D.W. Hess, et al., Relationship between work of adhesion and contact angle hysteresis on superhydrophobic surfaces, J. Phys. Chem. C 112 (30) (2008) 11403–11407.
[21] P. He, M. Huang, S. Fisher, et al., Effects of primer and annealing treatments on the shear strength between anodized Ti6Al4V and epoxy, Int. J. Adhesion Adhes. 57 (2015) 49–56.